



9th US National and 10th Canadian Conference on Earthquake
Engineering: *Reaching Beyond Borders*

toronto july 25-29, 2010

9ième Conférence Nationale Américaine et 10ième Conférence
Canadienne de Génie Parasismique: *Au delà des Frontières*

Conference Co-Sponsors
Earthquake Engineering
Research Institute

The Canadian Association for
Earthquake Engineering

L'Association Canadienne du
Génie Parasismique

EXPERIMENTAL DAMAGE-TRANSPORT CORRELATIONS FOR UNIAXIALLY- LOADED REINFORCED CONCRETE WALLS

Soppe, T.¹ and Hutchinson, T.C.²

ABSTRACT

In this paper, we experimentally evaluate the relationship between concrete damage and air flow using model-scale reinforced concrete walls. Herein, we focus on the walls behavior under uniaxial loading conditions. The method for evaluating the damage-flow rate relationship includes structural testing of scaled specimens, damage identification, and air flow rate experiments. Concrete damage is characterized on a local and global level, via consideration of crack characteristics (length and width) and drift ratio, respectively. Nine model specimens were tested, with variations in geometry, material, and loading details. All specimens had a well defined region of interest for damage identification and air flow testing. Air flow tests, in the form of pressure decay tests, were used to measure the concrete's permeability at different loading stages.

Introduction

Much of the hazardous material generated in the United States is stored in unlined concrete storage containers comprised of concrete shear walls. Concrete provides an exceptional barrier for containment storage; however, it is susceptible to leakage. Containment structures may be subjected to large lateral load demands due to earthquake and will likely crack. Once cracked, it is important to understand how much contaminant may leak into the environment. This combination of potential for cracking under even normal design conditions and large flow potential upon crack development has only been studied to a limited extent. The majority of research conducted on concrete permeability (a direct indicator of flow potential) focuses on uncracked permeability, which is an indicator of corrosion resistance. Corrosion resistance is an important property to quantify when determining the design life and serviceability of a structure. However, uncracked concrete typically has very low permeability and once cracked the permeability can increase by as much as 40 times (Girrens and Farrar, 1991).

Studies of leakage rates through cracked concrete started as early as the 1970's. Buss (1972) was likely the first to examine the effects of leakage through cracks in concrete. Following Buss's research, subsequent research has focused on the development of leakage rate formulas. Studies include for example; Rizkalla et al. (1984), Mayrhofer et al. (1988), Suzuki et al. (1989 and 1992), Girrens and Farrar (1991), Greiner and Ramm (1995), Riva et al. (1999), and Hamilton et al. (2004).

¹ Staff Engineer at W.E. Gundy & Associates, Inc

² Associate Professor, University of California, San Diego, La Jolla, CA

Scope of this Work

There remains limited experimental documentation on the leakage characteristics of cracked concrete components. Review of the literature indicates that previous tests have primarily focused on one or two variables, with lack of systematic consideration of a broad variety of wall characteristics that exist in practice. In this work, we systematically vary specimen characteristics while subjecting each specimen to combined structural uniaxial loading and flow rate experiments. Additional details of the study may be found in Soppe et al. (2008).

Experimental Program

Test Matrix

In this program nine specimens were tested under cyclic axial compressive and tensile loading with the anticipation of tensile splitting failure of the concrete (Fig. 1). Horizontal cracks were desired to provide well defined failure patterns and easily perform air flow tests. All nine specimens shared the same width and height measurements of 28 by 34 inches, respectively (Fig. 2). The remaining wall properties; thickness, unconfined uniaxial compressive strength f'_c , and vertical reinforcement ratio ρ_v were varied to study the effects each had on the measured air permeability. In addition to variations in wall properties, the loading protocol was also varied (Fig. 3).

Specimen thickness was varied from 3 inches to 6 inches in specimens U3 and U4, respectively. Specimens U1 and U2 were intended to vary concrete strength with target compressive strengths of 2500 psi and 6000 psi, respectively. Reinforcement ratio was halved in specimen U5 and doubled in specimen U6. Note that reinforcing bars for each specimen were placed in the center of the wall and were used to apply the tensile load to the specimen. Specimen U7 shared the same properties as specimen U0 but was tested under a different loading protocol. A baseline specimen was tested at the onset of the program (U0) and at the completion of the test program (U8).

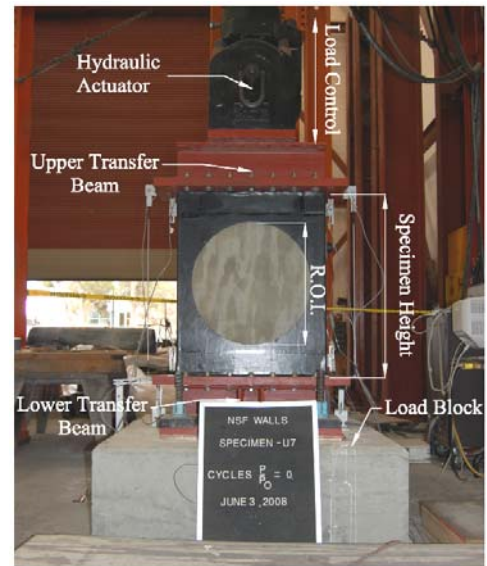


Figure 1. Photograph of test setup.

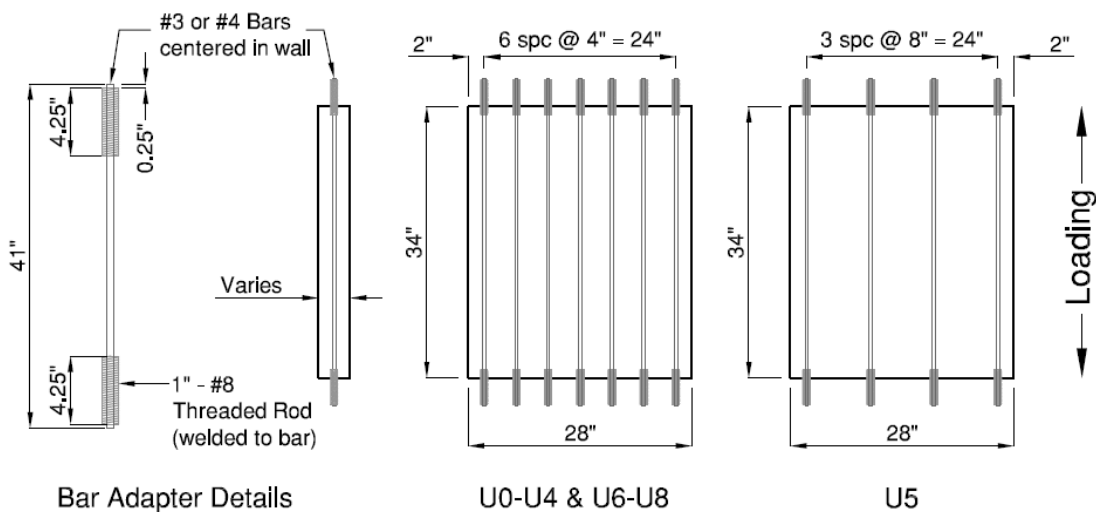


Figure 2. Specimen details.

The test program variables, concrete day of test (DOT) uniaxial compressive strength f'_c , and the estimated specimen tensile strength P_o are summarized in Table 1. Note that the specimen tensile strength P_o was estimated using the ACI 318-02 (2002) suggested expression. Three concrete mix designs were used in the construction of all nine specimens. All three mixes shared the same combination of Type II / V Portland cement, Flyash, 1/2" coarse gravel, 3/8" course gravel, sands, and water. The difference in concrete strengths between each mix design was achieved by modifying the w/c ratios. The three mix designs had w/c ratios of 0.33, 0.41, 0.51 corresponding to the three target concrete strengths of $f'_c = 2500\text{psi}$, 4000psi , and 6000psi respectively.

Table 1. Uniaxial specimen test matrix

Variable of Interest	Specimen No ¹	Test Dates 2008	Target Concrete strength f'_c [psi]	DOT Concrete strength f'_c [psi]	Panel Thickness [in]	Vertical Reinforcing Steel Ratio ρ_v ²	Loading Protocol ³	Estimated P_o [kips]
Baseline I	U0 ^a	2/11 - 2/14	4000	5318	4	0.69%	IA	58.5
Concrete Strength	U1 ^a	2/25 - 2/26	2500	3270	4	0.69%	IA	52.7
	U2 ^b	4/21 - 4/23	6000	7684	4	0.69%	IB	65.2
Panel Thickness	U3 ^b	5/7 - 5/12	4000	7012	3	0.92%	IB	45.0
	U4 ^c	5/28 - 5/30	4000	4754	6	0.46%	IB	85.4
ρ_v	U5 ^a	3/3 - 3/5	4000	5210	4	0.39%	IA	56.2
	U6 ^b	5/13 - 5/20	4000	7010	4	1.25%	IB	60.7
Loading Protocol	U7 ^c	6/3 - 6/6	4000	4982	4	0.69%	II	58.5
Baseline II	U8 ^c	6/10 - 6/12	4000	4989	4	0.69%	IB	58.5

¹ Due to imperfections in the initial constructed specimens, select specimens were re-poured, as a result three groups were cast, denoted a, b, and c above.

² $\rho_v = 0.69\%$, 0.92% , 0.46% = 7 - #3 bars, $\rho_v = 0.39\%$ = 4 - #3 bars, $\rho_v = 1.25\%$ = 7 - #4 bars

³ Loading Protocol IA was modified, indicated by IB, to prevent vertical compressive cracks. See Fig. 3.

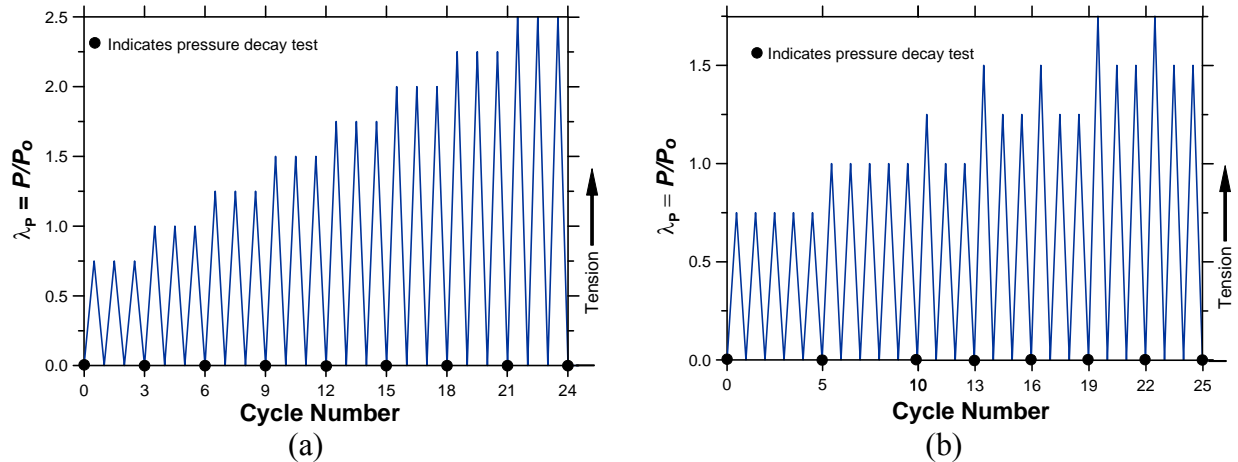


Figure 3. Load protocols used during testing: (a) protocol IB (modified ACI, 2004) and (b) protocol II (modified CUREE, 2001).

Loading Protocols

Cyclic axial loading was applied to the specimens under load control using three load protocols; (IA) ACI (2004) suggested protocol, (IB) modified ACI (2004) protocol and (II) a protocol suggested by CUREE (Krawinkler et al., 2001). All three loading protocols cycled about a precompressive (service level) axial load $N = 10\%f'_c A_g$, where, f'_c = target 28-day uniaxial compressive strength, and A_g = gross cross-sectional area of concrete. Peak amplitudes for each cycle were selected as fractions λ_p of the specimen design tensile strength P_o :

$$P_o = 7.5\sqrt{f'_c} A_c + A_s E_s \frac{7.5\sqrt{f'_c}}{E_c} \quad [\text{units: in-lb}] \quad (1)$$

where, A_c = cross-sectional area of concrete, A_s = total area of steel in section, E_s = steel modulus of elasticity, and E_c = concrete modulus of elasticity. It is important to point out that loading of the specimen cycled about a precompressive load N which caused the initial cycle to be entirely in compression.

Air Flow Testing

Pressure decay testing (PDT) was used to measure the intrinsic permeability k (otherwise referred to as permeability) of the concrete specimen at the conclusion of each load step, as noted in Fig. 3. The pressure decay test measures permeability by applying a differential pressure across an element and recording pressure, temperature, and the time it takes for the differential pressure to decay, in this case to atmospheric pressure. The relationship between permeability, temperature and decay time is governed by Darcy's Law (Wang, 2008; Soppe et al., 2008):

$$k = \frac{2\mu LVT_m \left(\frac{P_{t+\Delta t}}{T_{t+\Delta t}} - \frac{P_t}{T_t} \right)}{A\Delta t (P_{atm}^2 - P_m^2)} \quad (2)$$

where, μ = dynamic viscosity of air, L = length of concrete thru which air travels (wall thickness), V = volume of vacuum chamber, T_m = mean air temperature during test, P_t and $P_{t+\Delta t}$ = vacuum pressure at time t and $t + \Delta t$, T_t and $T_{t+\Delta t}$ = temperature at time t and $t + \Delta t$, A = area of concrete thru which air travels, Δt = time step duration, P_{atm} = atmospheric pressure, P_m = mean pressure. The PDT setup consists of a suction cup, vacuum pump, two pressure transducers, a thermocouple, three displacement transducers, and support frame (Fig. 4).

Results and Discussion

Global Response

The global response in terms of axial load versus displacement of all specimens is shown in Fig. 5. The primary axes of each graph represent the measured actuator load and specimen displacement, whereas the secondary axes (right and top) show the calculated global strain (measured specimen displacement divided by the specimen initial height) and load ratio (measured load normalized by design strength P_o). Also indicated on each graph is the point at which the observed first crack formed and consequentially the first cracked PDT was performed.

The response of all nine specimens was that typical of loading reinforced concrete in simple compression and tension. When loading in tension the system softens and large displacements are observed due to the straining of the reinforcement. Whereas, when loading in compression the system is extremely stiff and small displacements are observed. All nine specimens with the exception of specimens U4 and U5 approached their theoretical tensile design strength P_o . Specimens U4 and U5 did not reach the design tensile strength P_o because the strength of the reinforcement was less than P_o and once cracked the reinforcement strength controls the section capacity. Likewise, the strength provided by the reinforcement of specimens U3 and U6 was much greater than P_o , allowing the specimen to reach much higher load to design strength ratios (near 1.5). The remainder of specimens had reinforcement strengths that were similar to the overall design strength P_o which led to load to design strength ratios near 1.0.

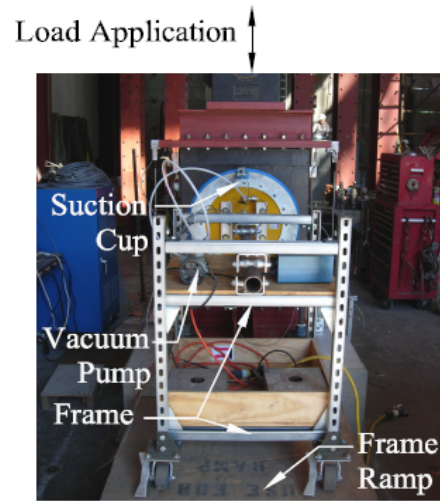


Figure 4. Pressure decay test setup

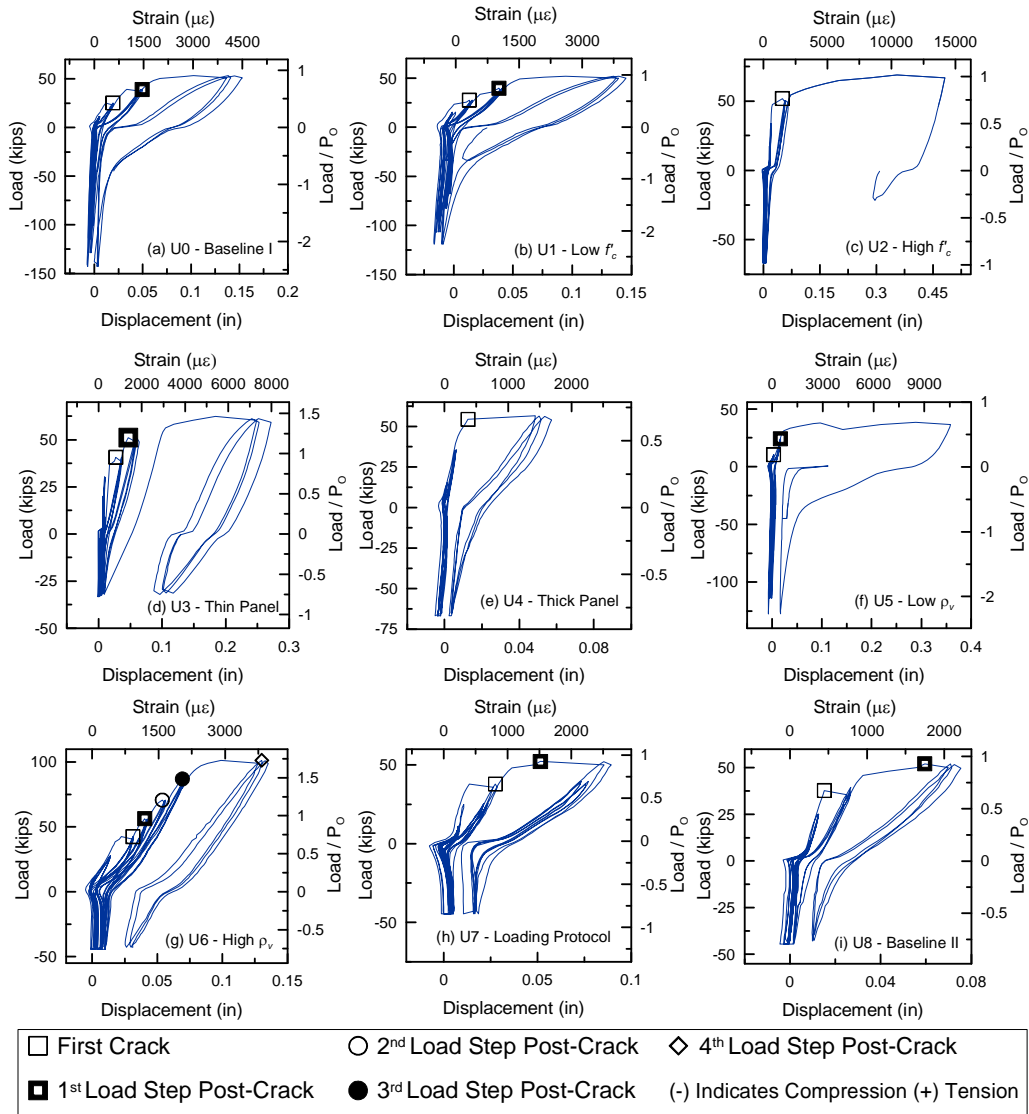
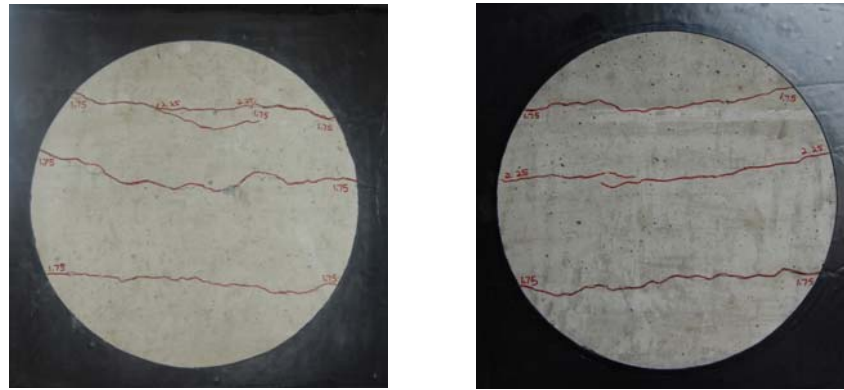


Figure 5. Specimen global response

Physical Observations

By way of example, damage observations for Specimen U3 are described. Specimen U3 was targeted to be identical to the baseline specimen with the exception of having a thinner wall panel (3 inch thickness). Under the first four load steps, $P/P_o = 0.75$, $P/P_o = 1.00$, $P/P_o = 1.25$, $P/P_o = 1.50$ there was no visible damage to specimen. The specimen first crack occurred during load level $P/P_o = 1.75$. The North face of the wall observed three cracks, while the South face presented only two at the surface. The randomness of concrete cracking is well known and one might anticipate the lack of visual symmetry of cracks on both faces due to a number of factors; e.g. uneven load application, poor local concrete vibration, and local debonding. The cracks on the North face were located at approximately 1/3, 1/2, and 3/4 of the height of the specimen with a crack spacing of approximately 6 inches. The cracks on South face were in similar location to that of the north face with the exception of the missing center crack, thus leaving a visible crack spacing of approximately 12 inches within the ROI. The cracks that propagated through both faces were of equal length within the region of interest. The average measured crack width of the top crack was 0.0006 inches on the North face and 0.0008 inches on the South face whereas the average bottom crack width was 0.0004 inches on the North face and 0.0013 inches on the South face. The average center crack width was 0.0008 inches on the North face. At the last viable load level for this specimen $P/P_o = 2.25$, the center crack propagated to the south face. As can be seen in Fig. 6, all three cracks remained the same length but likely widened due to the fact that a

vacuum could not be formed on the wall. Due to the widened crack widths, permeability tests could no longer be performed and crack widths were not measured.

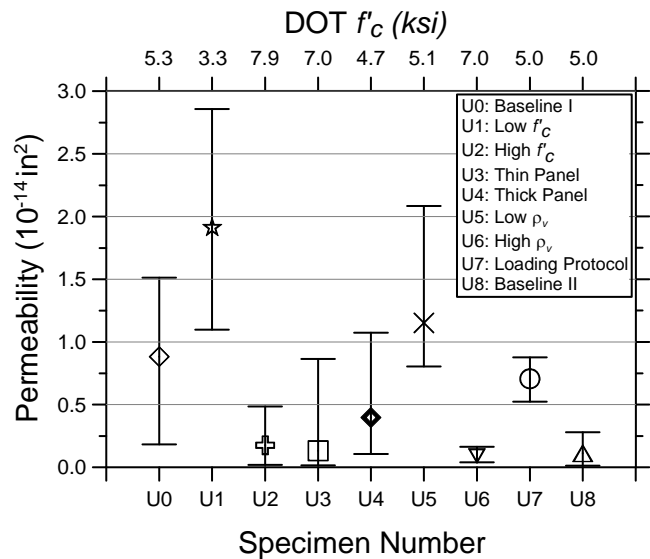


North Face
South Face
Figure 6. Specimen U3 at load step P/Po = 2.25

Uncracked Concrete Permeability

To determine a baseline uncracked permeability value a minimum of three pressure decay tests were performed prior to testing and two tests were performed after each load step prior to the specimen cracking. These tests indicated that the concrete permeability was unaffected by the applied load prior to cracking. Therefore, the permeability values calculated for all PDT's prior to cracking were averaged to establish the baseline uncracked concrete permeability. The average, minimum, and maximum uncracked permeability values for each specimen are shown in Fig. 7. The majority of the uncracked permeability values measured for each specimen were within the range of published values from $8.0 \times 10^{-15} \text{ in}^2$ to $4.0 \times 10^{-13} \text{ in}^2$ (Girrens and Farrar, 1991).

The largest influence on permeability for an uncracked concrete specimen is concrete strength, which is directly related to the water to cement ratio w/c . Higher concrete strengths are achieved using lower w/c ratios and lower strengths are attained using higher w/c ratios. The w/c ratio affects the amount of voids present in concrete; higher w/c ratios result in increased void ratios whereas lower w/c ratios reduce void content. Increased voids in concrete will result in increased air permeability, therefore it is expected that lower strength concrete (high w/c ratio) will have larger air permeability and high strength concrete (low w/c ratio) will be less permeable.



*Error bars delineate minimum and maximum values
Figure 7. Uncracked concrete permeability

Average permeability values and their corresponding DOT concrete strength shown in Fig. 7 are fairly consistent with the relationship between concrete strength and air permeability. The most permeable specimen was the specimen with the lowest concrete strength U1. The high strength concrete specimens U2, U3, and U6 all had the lowest measured permeable values. Specimens U0, U4, U5, U7 and U8 had concrete strengths near 5.0 ksi and had uncracked permeability values ranging from 1.2 to 1.1×10^{-15} . Although there are variations for these specimens, for example, panel thickness and vertical reinforcing ratio, given the small value of the numbers and range in permeability measurements, this range may be attributed to specimen to specimen variability.

Cracked Concrete Permeability

Fig. 8 shows the calculated average permeability versus load step for all nine specimens. The first observation made is that specimens U1, U4, U6, and U7 had the greatest measured (cracked) permeability and that their largest k values occurred at varied load steps. Specimen U1 was constructed of low strength concrete which also had the highest uncracked permeability. Specimen U4 varied in thickness (thickest specimen) and also had minimal reinforcement. Specimen U7 had the same properties as the baseline specimen but was loaded using a different loading protocol (more cycles).

Only specimens U2 and U6 (for load levels below $P/P_o = 2.50$ for U6) observed final cracked concrete permeability values less than 1.0×10^{-13} in². The lower permeability values are expected in specimen U6 because the specimen's reinforcement ratio was significantly larger than all other specimens resulting in better crack control. Specimen U2 was constructed with high strength concrete and had very low uncracked permeability. These results indicate that low concrete strength, low reinforcement ratio, and loading protocol have the greatest effect on increasing the overall (cracked) permeability of the specimen whereas the concrete permeability is best controlled using high reinforcement ratio and higher strength concrete.

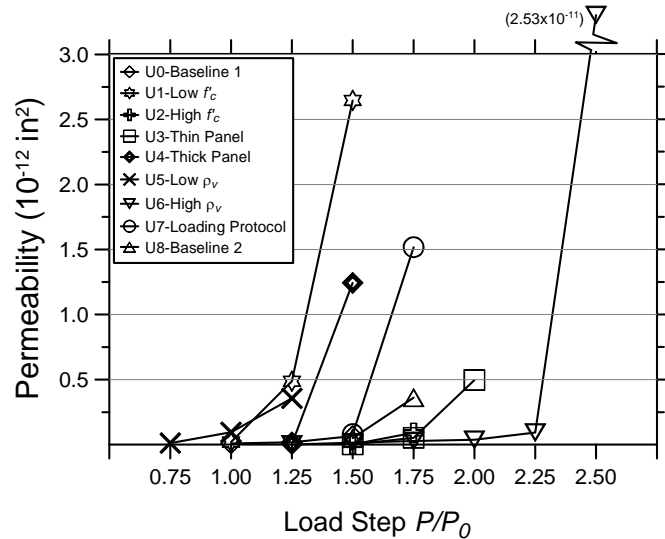


Figure 8. Permeability versus load step

The primary focus of this work is to study the effects of concrete strength, reinforcement ratio, concrete thickness, and loading protocol on the *cracked* concrete air permeability. For this reason, the normalized permeability k^* ($= k_{cracked}/k_{uncracked}$) is evaluated in detail, where, $k_{cracked}$ = the average measured cracked permeability and $k_{uncracked}$ = average uncracked permeability. Normalized permeability values measured after the first crack observed for each specimen are shown in Fig. 9. Note that the first crack occurred at load ratios ranging from $P/P_o = 1.0$ to 1.75 , for all of the specimens. All nine specimens, with the exception of specimen U5, cracked in the desired horizontal fashion. Specimens U0, U1, U4, U7, and U8 formed a single horizontal crack whereas specimens U2, U3, and U6 formed two or more initial cracks simultaneously. Specimen U5 formed a small vertical crack under load step $P/P_o = 1.0$ and due to this variation in crack development, is not directly comparable to the other specimens. Also, the first crack of specimen U0 was only visible on one face of the specimen and did not penetrate thru the entire thickness. Therefore, the results at first crack of specimen U0 is not as directly comparable to the remainder of the specimens.

Excluding specimens U0, U4, and U5, the normalized permeability at first crack ranges between 10 and 50. The permeability of specimen U4 at first crack is nearly 320 times that of the uncracked permeability and is more than 6 times greater than the permeability at first crack for any other specimen. The higher permeability at first crack for specimen U4 can be attributed to the low reinforcement ratio and wall thickness. The design thickness of the specimen was 6 inches and the reinforcement ratio was 0.46%. The thicker wall resulted in an increase in tensile strength P_o , therefore the specimen's first crack occurred at a larger applied load. Normalized permeability values shown in Fig. 9b indicate that concrete strength does not have a significant effect on the permeability of the specimen after first crack. No trend in k^* is observed when comparing the high strength (U2, U3, and U6), low strength (U1), and normal strength (U0, U4, U5, U7, and U8) concrete specimens.

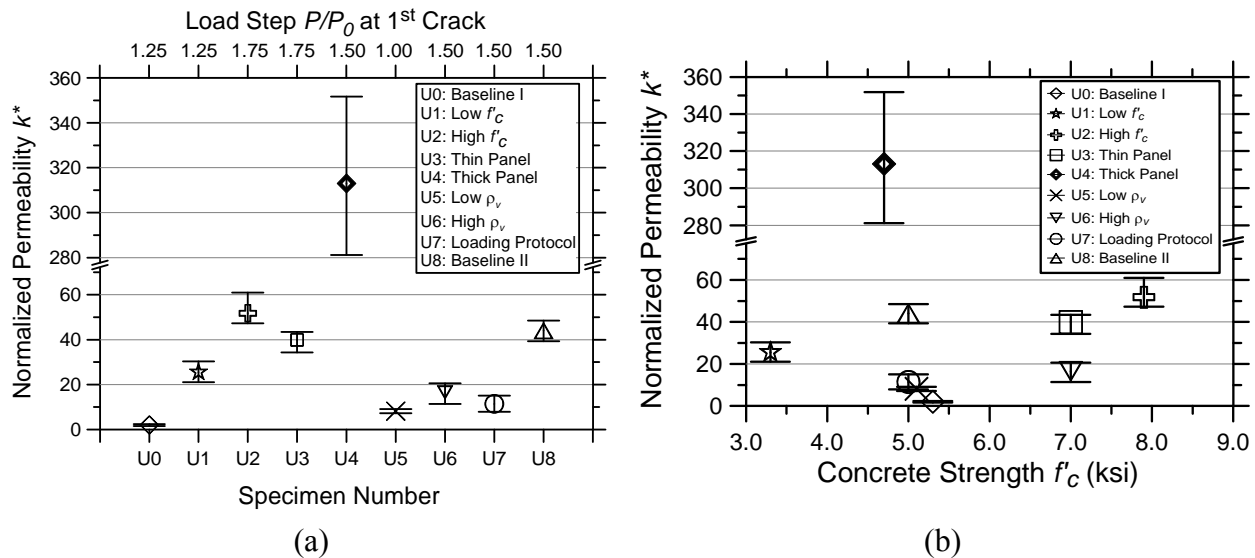


Figure 9. First crack normalized permeability: (a) per specimen and (b) versus DOT f'_c .

To evaluate the effects of wall thickness, one may compare specimens U4 and U5 or U3 and U6. Comparing specimens U5 and U4, both specimens have similar (low) reinforcement ratios and similar concrete strengths (near 5 ksi) but vary in thickness (6 in and 4 in). This comparison indicates that the thicker wall (U4) is more permeable after the first crack relative to its uncracked permeability. The second set of specimens that can be compared is U3 and U6, both specimens have the same reinforcement ratios and similar concrete strengths (near 7 ksi) but U3 is 3 inches thick and U6 is 4 inches thick. This comparison indicates that the thinner wall (U3) is more permeable at first crack than the thicker wall relative to its uncracked permeability. When looking at both comparisons of the actual and normalized permeability shown in Figs. 8 and 9, respectively, both sets of data contradict each other and therefore no definitive statement regarding the effects of wall thickness can be made.

Loading protocol effects were evaluated by comparing specimens U7 and U8. Specimen U7 and U8 had the same thickness, reinforcement ratio, and were constructed with the same concrete mix. Also both specimens attained their first crack at load step $P/P_o = 1.50$. When subjected to different loading protocols, the normalized permeability at first crack for specimen U8 was three times larger than the normalized permeability for specimen U7. However, the baseline uncracked permeability for specimen U7 was approximately six times greater than that of specimen U8, which would tend to cause the calculated normalized permeability to be much smaller. If both specimens had the same baseline uncracked permeability, specimen U7 would have greater cracked normalized permeability values than U8. Also, when looking at the permeability values (Fig. 8), it is apparent that specimen U7 has a much higher permeability than U8 at the same load levels. This comparison indicates that as expected the greater number of load cycles (varied loading protocol) tends to increase the cracked concrete permeability.

When observing the normalized permeability values for the specimens under subsequent load cycles beyond first crack, select specimens observe significant increases in k^* , while others do not. To help understand why the permeability increased substantially for some specimens and not in others, a graph of the normalized permeability versus cracked surface area is shown in Fig. 10. The cracked surface area represents to total cracked area on one face of the specimen and was calculated by averaging the measured crack area (length x width) of each face of the specimen as observed at each load step. All specimens indicate an increase in cracked surface area with increasing load amplitude thus resulting in an increase in normalized permeability. The trend appears to be exponential in nature with larger increases in permeability at later load steps for the same increases in cracked surface area. The largest permeability increase seen with specimen U6 is attributed to the greatest increase in cracked surface area. This is also the case with specimens U7, U3 and U8. The data shown for specimen U6 up to load step $P/P_o = 2.25$

doesn't follow the same trend in that there was not as great of an increase in permeability for the similar increase in cracked surface area. This may be due to the very high concrete strength of this specimen ($f'_c = 7$ ksi) and large vertical steel reinforcement ratio ($\rho_v = 1.25\%$).

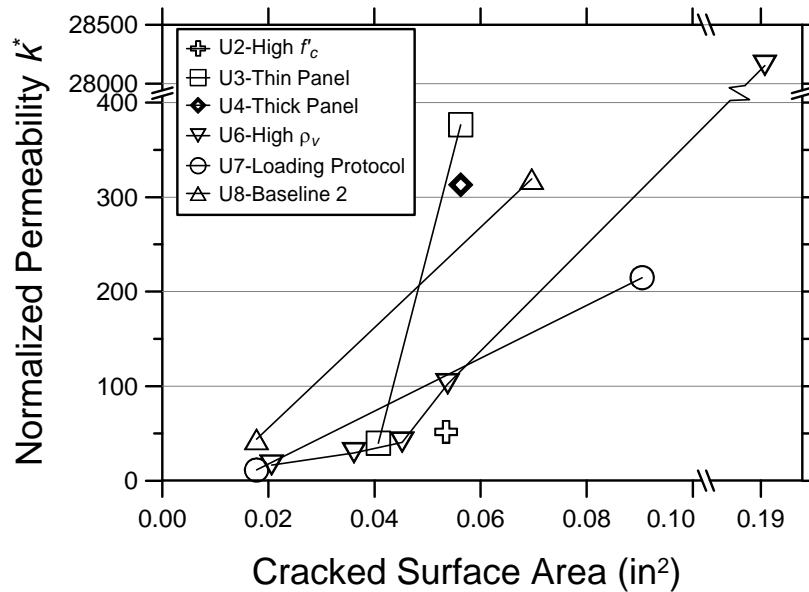


Figure 10. Normalized permeability versus cracked surface area

Conclusions

The relationship between concrete damage (cracking) and gas flow (permeability) has been largely unexplored. In the design of nuclear or hazardous facilities, this may become a critical design parameter, particular as damage to structural components (walls in this case) develops under seismic loading. In this work, the relationship between damage and/or load and permeability is experimentally investigated, using model scale reinforced concrete wall panels. Unlike most prior efforts, the emphasis was on characterizing this flow for cracked specimens, in other words, correlating flow with the progression of damage. Nine model specimens were tested, with variations in concrete strength, wall thickness, reinforcement ratio, and loading protocol. Each specimen was subjected to cyclic uniaxial loading, identification and characterization of cracks, and finally execution of air flow rate experiments at varied load steps. Results from the air flow rate experiments were then compared with values calculated using existing air flow rate formulae.

Air flow tests were performed on the specimen in both the uncracked and cracked state. The uncracked permeability's measured were within the range of published values in the literature. The most significant influence on the uncracked permeability is the concrete strength. The specimen with the lowest concrete strength (U1 - DOT $f'_c = 3270$ psi) had an uncracked permeability that was approximately 11 times greater than the uncracked permeability of the specimen with the highest concrete strength (U2 - DOT $f'_c = 7684$ psi).

Once cracked, the concrete permeability typically increased anywhere from 10 to 50 times the uncracked permeability. In some cases, very large post crack permeability's were observed, on the order of 300-400 times that of the uncracked permeability. These larger values were primarily observed at the later load stages, when multiple cracks were observed and the first cracks had significantly widened. The largest cracked concrete permeability's (as measured at the same load step) were observed in specimens with low concrete strength, low reinforcement ratio, and with varied loading protocol (greater number of cycles). Whereas, the lowest cracked concrete permeability values were found in specimens with high strength concrete and a high reinforcement ratio. These results indicate that the most suitable method for controlling (minimizing) flow through wall panels expected to crack is to design a specimen with a high

reinforcement ratio and use high strength concrete. This design suggestion is intuitive because a greater amount of reinforcement will help to bridge and control crack development, while a larger concrete strength will have a higher tensile strength thus requiring larger loads to induce cracking.

Acknowledgements

This work was supported by the National Science Foundation (NSF) under grant number CMMI-0729357, where Dr. Jorn Larsen-Basse and Dr. Lawrence Bank are the program managers. Special thanks to Dr. Ting Wang who assisted with the initial specimen design and construction, and the UCSD Powell Laboratory staff, in particular, Dr. Chris Latham, Mr. Andy Gunthardt, and Mr. Bob Parks. The above support is greatly appreciated. Opinions, findings, and conclusions expressed in this report are those of the authors, and do not necessarily reflect those of the sponsoring organization.

References

- ACI 318-02 (2002). Building code requirements for structural concrete (ACI 318-02) and commentary (ACI 318R-02). *American Concrete Institute*, Detroit, MI.
- Buss, W. (1972). "Proof leakage rate of a concrete reactor building." *Concrete for Nuclear Reactors ACI Special Publication Sp-34*, III , 1291-1320.
- Girrens, S. P., and Farrar, C.R. (1991). "Experimental assessment of air permeability in a concrete shear wall subjected to simulated seismic loading." *Los Alamos National Laboratory Report*, LA-12124-MS, Los Alamos, New Mexico.
- Greiner, U., and Ramm, W. (1995). "Air leakage characteristics in cracked concrete." *Nuclear Engineering and Design*, 156, 167-172.
- Hamilton, C.H., Hutchinson, T.C., Pardoen, G.C., Salmon, M.W., Wang, T., (2004). "Gas and aerosol leakage rate through reinforced concrete shear walls: experimental study." *Proceedings of the 13th World Conference on Earthquake Engineering*, Vancouver, B.C., Canada, No. 2484.
- Mayrhofer, C., Kornerk, W., Brugger, W., (1988). "Gas impermeability of reinforced concrete slabs supported on four sides." *Part 2. Foreign Technology Division Wright-Patterson AFB report FTD-ID(RS) T-0085-88*.
- Riva, P. B., Brua, L., Contri, P., and Imperato, L. (1999). "Prediction of air and steam leak rate through cracked reinforced concrete panels." *Nuclear Engineering and Design*, 192, 13-30.
- Rizkalla, S. H., Lau, B. L., and Simmonds, S. H. (1984). "Air leakage characteristics in reinforced concrete." *Journal of Structural Engineering ASCE*, 110(5), 1149-1162.
- Soppe, T., Stoehvase, M. and Hutchinson, T.C. (2008). Experimental Damage-Transport Correlations for Uniaxially-Loaded Reinforced Concrete Walls. Structural Systems Research Project Report Series. SSRP 08/07. Department of Structural Engineering, University of California, San Diego. La Jolla, California.
- Suzuki, T., Takiguchi, K., Hotta, H., Kojima, N., Fukuhara, M., and Kimura, K. (1989). "Experimental study on the leakage of gas through cracked concrete walls." *Proceedings of SMIRT-10*, Q, 145-150.
- Suzuki, T., Takiguchi, K., Hotta, H. (1992). "Leakage of gas through cracked concrete cracks." *Nuclear Engineering and Design*, 133, 121-130.
- Wang, T., (2008). "Gas leakage rate through low aspect ratio concrete shearwalls." PhD Dissertation. University of California, Irvine, Department of Civil Engineering.